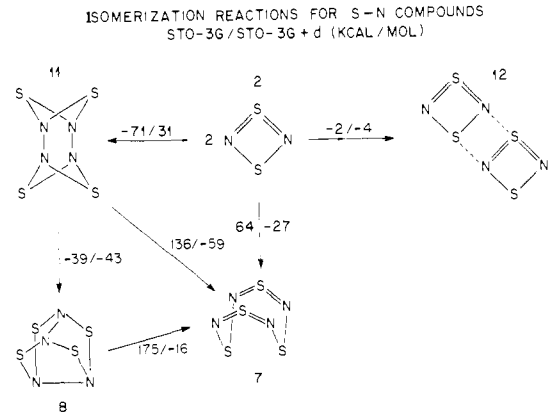

Figure 3. Highlights of the importance of d functions on sulfur in describing various bonding situations.

at the minimal basis set level and presumably results from dipolar bonding (cf. Figure 1a). Remote substituents therefore do not seem effective in increasing the participation of the d orbitals in bonding to sulfur via the hypervalent state. The results of the present study are not encouraging with respect to the prospects for the production of an $(HCS)_x$ polymer.

Conclusion

(i) With regard to energetic (and to some extent structural) comparisons between sulfur-containing molecules, the inclusion of d functions in the sulfur basis set is found to be (a) relatively unimportant in comparisons between structures containing only valent sulfur, (b) important in comparisons between molecules containing the same number of hypervalent sulfur atoms, and (c) mandatory in comparisons between molecules which contain unequal numbers of hypervalent sulfur atoms. These points are illustrated in Figure 3.

(ii) The conjugation energy of the linear N-S bond is found to be 8 kcal/mol at the minimal basis set level and 17 kcal/mol with the inclusion of d functions.

(iii) The hypervalent state of sulfur (with d-orbital participation) is only about half as effective in bonds to carbon as it is in bonds to nitrogen when energetic comparisons are made with valent isomers. This factor, together with the greater strength of the C-C single bond as against the N-N single bond, militates against the viability of $(SCH)_{2n}$-type structures.

Acknowledgment. We are grateful to M. L. Kaplan for many informative discussions and for comments on the manuscript.

Excitation Profiles, Absorption and Resonance Raman Spectra of the Carotenoprotein Ovorubin, and a Resonance Raman Study of Some Other Astaxanthin Proteins

Robin J. H. Clark,* Norman R. D'Urso, and Peter F. Zagalsky

Contribution from the Christopher Ingold Laboratories, University College London, London WC1H 0AJ, England, and the Department of Biochemistry, Bedford College, London NW1 4NS, England. *Received March 10, 1980*

Abstract: The resonance Raman spectrum of ovorubin, excited by irradiation within the contour of the lowest $\pi^* \leftarrow \pi$ absorption band, has been observed and compared to those of some other astaxanthin proteins. The excitation profiles and relative intensities of the three most intense bands in the resonance Raman spectrum of ovorubin, together with those of a number of their combination tones and overtones, have been measured and analyzed by using a simple model applied previously to free carotenoids. The results lead to estimates of the elongation of the C=C and shrinkage of the C—C bonds in the resonant excited state. The correlation, for ovorubin and a number of other astaxanthin proteins, between the ν_1 wavenumber and $1/\lambda_{max}$ of the $\pi^* \leftarrow \pi$ absorption band is investigated and discussed in terms of current ideas on the binding of astaxanthin in astaxanthin proteins.

Introduction

The carotenoid astaxanthin (I) has been shown to occur in a variety of carotenoproteins from invertebrates such as *Pomacea canaliculata* (ovorubin), *Hommarus gammarus*, and *Velella velella*.[1-4]

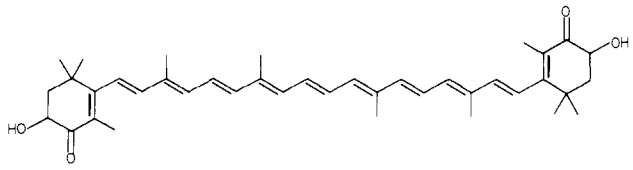

I

The visible absorption spectrum of free astaxanthin in organic solvents[5] shows a strong band at 480 nm; at low temperature this band exhibits vibronic structure. In common with that of other carotenoids the band is caused by a $\pi^* \leftarrow \pi$ type transition of the π electrons delocalized along the polyene chain.[6] On association of astaxanthin with protein, the absorption maximum may be subjected to large wavelength shifts.[1,2,4] The type of binding, the conformation of the carotenoid and the state of astaxanthin aggregates are important factors in the perturbation of the π-electron system and so may be expected to account for these shifts. In this respect, resonance Raman spectroscopy is an important analytical tool since the technique is capable of probing vibrational properties of a carotenoid, even if the latter is situated within carotenoproteins of large molecular weight.[7-12]

*To whom correspondence should be addressed at University College London.

(1) D. F. Cheesman, W. L. Lee, and P. F. Zagalsky, *Biol. Rev. Cambridge Philos. Soc.*, **42**, 131 (1967).
(2) P. F. Zagalsky, *Pure Appl. Chem.*, **47**, 103 (1976).
(3) D. F. Cheesman, *Proc. Roy. Soc. London, Ser. B* **149**, 571 (1958).
(4) O. Isler, Ed., "Carotenoids", Halsted Press, New York, 1971.
(5) V. R. Salares, R. Mendelsohn, P. R. Carey, and H. J. Bernstein, *J. Phys. Chem.*, **80**, 1137 (1976).
(6) J. Dale, *Acta Chem. Scand.*, **8**, 1235 (1954).

0002-7863/80/1502-6693$01.00/0

The wavenumber of the Raman-active vibration (ν_1) (essentially a C=C stretch) is also particularly sensitive to the protein environment of the carotenoid.[7,8] If the only factor affecting the electronic spectral properties of the astaxanthin were the extent of π-electron delocalization along the chain, then a direct correlation would be expected between the Raman and absorption shifts.[10,11] However, if other factors are important, then the relationship may be complicated since the Raman band wavenumber is an electronic ground-state property, whereas the absorption spectrum is a property of both the ground as well as the excited states.

The red carotenoprotein ovorubin, obtained from the eggs of the snail *Pomacea canaliculata australis*, contains one astaxanthin unit per molecule (M = ca. 330000).[3] Its lowest $\pi^* \leftarrow \pi$ transition (λ_{max} = 508 nm) is particularly well suited to detailed resonance Raman studies since the associated absorption band exhibits vibronic structure even at room temperature. The relative intensities of these vibronic components are dependent on the displacements of the excited-state potential minima from that of the ground state along certain totally symmetric normal coordinates. These displacement parameters also control, inter alia, the relative Raman intensities of the totally symmetric modes and their excitation profiles (variation of Raman band intensities with excitation wavenumber

In this study the displacement parameters from the absorption spectrum of ovorubin have been taken as starting values and used to simulate the excitation profiles and relative intensities of a number of intense Raman bands of the carotenoid. Refinement of the fit between calculated and observed excitation profiles has then led to refined values for the displacement parameters.

The resonance Raman spectra of a red astaxanthin protein[13] from the eggs of a related species of snail, *Pomacea insularum*, and of the blue mantle astaxanthin protein of the Chondrophore, *Velella velella*, are also presented. The correlation between the ν_1 wavenumber and the $1/\lambda_{max}$ for these and other, previously investigated,[8] astaxanthin proteins is examined and discussed.

Theoretical Background

It has been shown that, for a number of carotenoids and polyenes, the potential minimum of the excited state involved in the $\pi^* \leftarrow \pi$ transition is displaced, relative to that of the ground state, along totally symmetric normal coordinates.[14,15] The excitation profiles of the Raman bands and the absorption band shape may then be predicted by considering appropriate vibrational overlap integrals in the Franck–Condon approximation.[5,14,16-19]

The orthogonality between excited- and ground-state harmonic vibrational wave functions may be removed in two ways:[20] (1) a shift of the excited-state potential minimum relative to that of the ground state along one or more normal coordinates; (2) a distortion of the excited-state potential relative to that of the ground state, resulting in a change of vibrational wavenumber.

For the model used in this study[5,16-19] only the first of these two mechanisms is taken into account. Considering initially a shift along one normal coordinate, the vibrational overlap integrals may be obtained from the recurrence relations (1)–(4) of Manneback[21]

$$\langle 0_g|v_e + 1\rangle = -\frac{M}{(v+1)^{1/2}}\langle 0_g|v_e\rangle \quad (1)$$

$$\langle n_g|v_e + 1\rangle = \left(\frac{n}{v+1}\right)^{1/2}\langle n_g - 1|v_e\rangle - \frac{M}{(v+1)^{1/2}}\langle n_g|v_e\rangle \quad (2)$$

$$\langle n_g + 1|0_e\rangle = \frac{M}{(n+1)^{1/2}}\langle n_g|0_e\rangle \quad (3)$$

$$\langle 0_g|0_e\rangle = \exp\left(-\frac{M^2}{2}\right) \quad (4)$$

where n, v, and 0 (the lowest) are vibrational quantum numbers and g and e represent ground and excited states, respectively. The quantity to be determined is the (dimensionless) displacement parameter M, which is a function of the vibrational frequency and of the displacement of the excited-state potential minimum relative to that of the ground state along the normal coordinate.

When the excited state is shifted along more than one normal coordinate, the vibrational overlap integrals become multidimensional, with each dimension being defined by an appropriate normal coordinate. Thus

$$\langle \bar{n}_g|\bar{v}_e\rangle = \langle (n_1 n_2 n_3 \ldots n_m)_g|(v_1 v_2 v_3 \ldots v_m)_e\rangle \quad (5)$$

where m is the number of normal coordinates along which the excited-state potential is shifted and $\langle \bar{n}\rangle$ is a multidimensional wave function.

By neglecting the change in shape of the molecule in the excited state, we may use the independent-mode approximation to reduce the multidimensional vibrational overlap integrals to the products of one-dimensional ones,

$$\langle \bar{n}_g|\bar{v}_e\rangle = \prod_{a=1}^{m}\langle n_{ag}|v_{ae}\rangle \quad (6)$$

The intensity of the absorption band at wavenumber $\tilde{\nu}$ is given by eq 7, where $\tilde{\nu}_{\bar{v}_e,\bar{0}_g}$ is the wavenumber of the vibronic transition

$$A(\tilde{\nu}) = k\sum_{\bar{v}_e}|\langle \bar{v}_e|\bar{0}_g\rangle|^2 \tilde{\nu}_{\bar{v}_e,\bar{0}_g} S(\bar{v}_e,\bar{0}_g) \quad (7)$$

$\bar{v}_e \leftarrow \bar{0}_g$ and $S(\bar{v}_e,\bar{0}_g)$ is a shape function containing the full-width at half-maximum (fwhm) of the vibronic band. The constant k involves the $\pi^* \leftarrow \pi$ transition moment. The value of k is not known, so eq 1 may be used only to calculate the profile but not the absolute intensity of the absorption band.

The general equation for the intensity of a Raman transition $\bar{n}_g \leftarrow \bar{0}_g$ is given by eq 8, where $\tilde{\nu}_0$ is the wavenumber of the exciting radiation, $\tilde{\nu}_{\bar{n}_g,\bar{0}_g}$ is the wavenumber of the Raman transition, and $\alpha_{\rho\sigma}$ is the $\rho\sigma$th element of the polarizability tensor.

$$I_{\bar{n}_g,\bar{0}_g} = \frac{2^7\pi^5}{3^2} I_0(\tilde{\nu}_0 - \tilde{\nu}_{\bar{n}_g,\bar{0}_g})^4 \sum_{\rho,\sigma}|(\alpha_{\rho\sigma})_{\bar{n}_g,\bar{0}_g}|^2 \quad (8)$$

In this study the excitation profiles are analyzed by using Albrecht's formulation[22] in which the polarizability tensor is given as the sum of two terms, A and B. As in previous work on carotenoids and polyenes, a number of simplifications to the general theory have been made: (1) Only one excited state, that involved in the $\pi^* \leftarrow \pi$ transiton, is in resonance. (2) Only the A (Franck–Condon) term need be considered. (3) Only one diagonal component (α_{zz}) of the polarizability tensor contributes to the A term since the Raman fundamentals to be considered were found to have depolarization ratios close to 1/3 on resonance.[23] Under these conditions, the square modulus of the transition polarizability in eq 8 may be written as eq 9, where $\bar{\nu}_{\bar{v}}$

(7) V. R. Salares, N. M. Young, H. J. Bernstein, and P. R. Carey, *Biochemistry*, **16**, 4751 (1977).
(8) V. R. Salares, N. M. Young, H. J. Bernstein, and P. R. Carey, *Biochim. Biophys. Acta*, **576**, 176 (1979).
(9) P. F. Zagalsky and P. J. Herring, *Philos. Trans. R. Soc. London, Ser. B*, **279**, 289 (1977).
(10) M. E. Heyde, D. Gill, R. G. Kilponen, and L. Rimai, *J. Am. Chem. Soc.*, **93**, 6776 (1971).
(11) L. Rimai, M. E. Heyde, and D. Gill, *J. Am. Chem. Soc.*, **95**, 4493 (1973).
(12) C. C. Shone, "Carotenoids and Carotenoproteins in Marine Invertebrates", Ph.D. thesis, University of Liverpool, 1978.
(13) B. A. Helm, unpublished results.
(14) A. Warshel and P. Dauber, *J. Chem. Phys.*, **66**, 5477 (1977).
(15) A. Warshel and M. Karplus, *Chem. Phys. Lett.*, **17**, 7 (1972).
(16) F. Inagaki, M. Tasumi, and T. Miyazawa, *J. Mol. Spectrosc.*, **50**, 286 (1974).
(17) A. V. Lukashin and M. D. Frank-Kamenetski, *Chem. Phys.*, **35**, 469 (1978).
(18) S. Sufra, G. Dellepiane, G. Masetti, and G. Zerbi, *J. Raman Spectrosc.*, **6**, 267 (1977).
(19) R. J. H. Clark, D. G. Cobbold, and B. Stewart, *Chem. Phys. Lett.*, **69**, 488 (1980).
(20) R. J. H. Clark and B. Stewart, *Struct. Bonding (Berlin)*, **36**, 1 (1979).
(21) C. Mannebach, *Physica (Amsterdam)*, **17**, 1001 (1951).
(22) A. C. Albrecht, *J. Chem. Phys.*, **34**, 1476 (1961).
(23) S. Hassing and O. Mortensen in *Adv. Infrared Raman Spectrosc.*, **6**, 1 (1980).

$= \tilde{\nu}_{eg} + \tilde{\nu}_{\bar{v}\bar{0}} - \tilde{\nu}_0$, $|\mu_z^0|_{eg}$ = electronic transition dipole moment in the z direction, and $\Gamma_{\bar{v}}$ = a damping factor, which is taken to be equal to the fwhm of a vibronic component of the absorption spectrum. The second summation represents the cross terms between different vibrational levels $\bar{v}$ and $\bar{u}$.

$$|\alpha_{zz}|_{\bar{n}_g,\bar{0}_g}^2 = \frac{|\mu_z^0|_{eg}^2}{h^2c^2}\left[\sum_{\bar{v}}\frac{(\langle\bar{n}_g|\bar{v}_e\rangle\langle\bar{v}_e|\bar{0}_g\rangle)^2}{(\tilde{\nu}_{\bar{v}}^2 + \Gamma_{\bar{v}}^2)} + 2\sum_{\bar{v}<\bar{u}}\sum\frac{\langle\bar{n}_g|\bar{v}_e\rangle\langle\bar{v}_e|\bar{0}_g\rangle\langle\bar{n}_g|\bar{u}_e\rangle\langle\bar{u}_e|\bar{0}_g\rangle(\tilde{\nu}_{\bar{v}}\tilde{\nu}_{\bar{u}} + \Gamma_{\bar{v}}\Gamma_{\bar{u}})}{(\tilde{\nu}_{\bar{v}}^2 + \Gamma_{\bar{v}}^2)(\tilde{\nu}_{\bar{u}}^2 + \Gamma_{\bar{u}}^2)}\right] \quad (9)$$

For the fundamental Raman transitions of the mth mode, the multidimensional overlap integrals become $\langle\bar{n}_g|\bar{v}_e\rangle = \langle 1_{mg}|v_{me}\rangle \cdot \Pi_{a-1}^m\langle 0_{ag}|v_{ae}\rangle$, $\langle\bar{v}_e|\bar{0}_g\rangle = \Pi_{a-1}^m\langle v_{ae}|0_{ag}\rangle$, and $\tilde{\nu}_{\bar{v}\bar{0}} = \tilde{\nu}(v_1\nu_1 + v_2\nu_2 + \ldots + v_m\nu_m)$. For the first overtone, we have $\langle\bar{n}_g|\bar{v}_e\rangle = \langle 2_{mg}|v_{me}\rangle\Pi_{a-1}^m\langle 0_{ag}|v_{ae}\rangle$, and for a binary combination band involving the mth and pth modes $\langle\bar{n}_g|\bar{v}_e\rangle = \langle 1_{mg}|v_{me}\rangle \cdot \langle 1_{pg}|v_{pe}\rangle\Pi_{a\neq m,p}\langle 0_{ag}|v_{ae}\rangle$.

With use of these relationships, computer programs were written to calculate absorption and excitation profiles. The following assumptions were made: (1) The shape function used in eq 1 was assumed to be Lorentzian since the theoretical model used does not justify further refinement. (2) The half-bandwidths (fwhm) used were taken to be the same for each vibronic level. (3) The summations were truncated when further terms were found to have a negligible effect on the calculated intensities, viz., when (a) $|\tilde{\nu}_{\bar{v}_e\bar{0}_g} - \tilde{\nu}_0| > 10^5$ cm^{-1} and/or (b) $10^6\langle n|v\rangle < \langle n|v\rangle_{max}$.

Experimental Section

Ovorubin was prepared as described in ref 3.

Raman Spectra. Raman spectra were recorded on a Spex 1401 double monochromator equipped with a cooled RCA-C31034A photomultiplier, photon counting detection with linear display, and 90° scattering geometry. Coherent Radiation Model 52 Kr^+ and Ar^+ lasers provided the exciting radiation.

The spectra, all at room temperature, were obtained from stationary samples of an aqueous solution of ovorubin buffered with 0.1 M tris/HCl (pH 6.5), using the 1354-cm^{-1} band of sodium formate (ca. 3 M) as an intensity standard (tris = tris(hydroxymethyl)methylamine). Laser powers of, typically, 100 mW were employed, and a bracketing procedure used to check that no thermal degradation of the sample had occurred was also employed.

Intensities were obtained from peak heights and half-bandwidths (fwhm) and are considered accurate to ±10%. The data were corrected for the spectral response of the spectrometer and for frequency-dependent factors.

The intensity of the 1354-cm^{-1} band of sodium formate was measured relative to that of the 981-cm^{-1} band of sodium sulfate for exciting radiation ranging from 530.9 to 457.9 nm. The relative intensity remained constant within experimental error.

Raman band wavenumbers were calibrated by using neon emission lines. All measurements were repeated at least three times.

Absorption Spectra. Absorption spectra were measured with the use of a Cary 14 spectrophotometer and 1-mm path length solution cells.

Results

Absorption Spectra. The room-temperature absorption spectrum of ovorubin shows fine structure[3] in the $\pi^* \leftarrow \pi$ band which is comparable to that obtained for the astaxanthin monomer in EPA at −162 °C.[5] However, at room temperature, astaxanthin itself has an absorption spectrum devoid of vibronic structure, suggesting that the greater detail observed in that of ovorubin is due to a decrease in the extent of the relaxational mechanisms that affect the half-bandwidths of the vibronic components. This may be caused, as suggested for the carotenoprotein ovoverdin, by two effects:[8] (1) isolation of the astaxanthin by the protein from the solvent environment; (2) constraints placed on the conformation of the carotenoid by being bound to the protein.

Raman Spectra. The resonance Raman spectrum of ovorubin is shown in Figure 1a. All the observed vibrational band wavenumbers are listed in Table Ia,b, together with previous data relating to the 500–1600-cm^{-1} region for the astaxanthin molecule. Also included in Table Ia are the recently reported wavenumbers of vibrational bands of several other astaxanthin proteins.

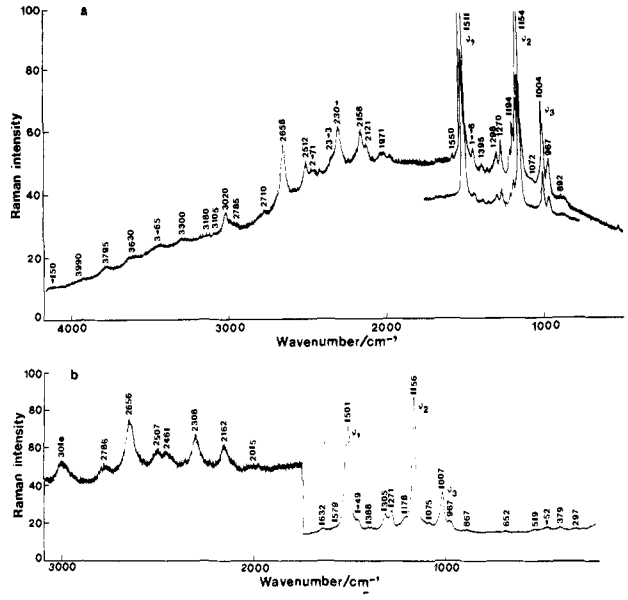

Figure 1. (a) Resonance Raman spectrum of ovorubin, taken on a capillary sample using 530.9-nm excitation at 30 mW: spectral slit width = 4 cm^{-1}, scan speed = 100 cm^{-1} min^{-1}, time constant = 0.25 s, scale = 50 K (inset 100 K). (b) Resonance Raman spectrum of *Velella velella* (λ_{max} = 620 nm) using 647.1-nm excitation at 400 mW: spectral slit width = 4 cm^{-1}, scan speed = 100 cm^{-1} min^{-1}, time constant = 0.4 s, scale = 10 K (overtone region) and 50 K (fundamental region).

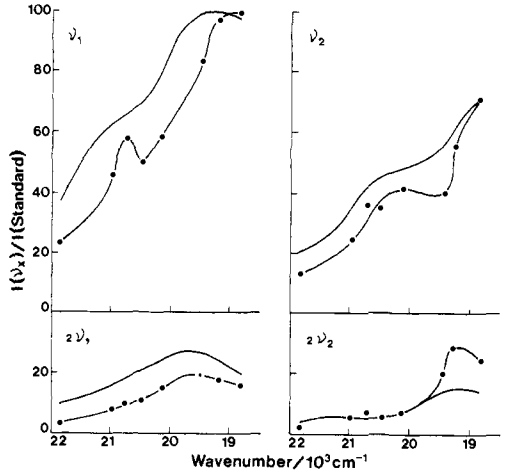

Figure 2. Observed (●) and calculated excitation profiles of the ν_1, $2\nu_1$, ν_2, and $2\nu_2$ bands of ovorubin. The experimental data are given relative to the intensity of the 1354-cm^{-1} band of sodium formate as internal standard.

Table Ia shows the astaxanthin proteins to have many more vibrational bands than free astaxanthin.[7] Although this would not seem surprising in view of the complexity of the biochemical system, there is considerable experimental[11,24] and theoretical[14] work on polyene derivatives to indicate that the extra bands are, in fact, attributable to the astaxanthin part of the molecule in each case rather than to the protein. Possible assignments for these bands, based largely on those for vitamin A derivatives and their protein complexes,[25-27] are also given in Table I.

There is a close correspondence between the wavenumbers of corresponding bands of ovorubin and of other astaxanthin proteins.

(24) R. Callender and B. Honig, *Annu. Rev. Biophys. Bioeng.*, **6**, 33 (1977).
(25) R. E. Cookingham, A. Lewis, and A. T. Lemley, *Biochemistry*, **17**, 4699 (1978).
(26) V. R. Salares, N. M. Young, P. R. Carey, and H. J. Bernstein, *J. Raman Spectrosc.*, **6**, 282 (1977).
(27) M. A. Marcus and A. Lewis, *Biochemistry*, **17**, 4723 (1978).

Table I

(a) Vibrational Band Wavenumbers (300–1600-cm^{-1} Region) of Some Astaxanthin Proteins[a]

astaxanthin in acetone[b]	ovorubin	*P insularum* astaxanthin protein[g]	V_{620}[h]	ovoverdin[i]		α-crustacyanin[j]	assignt
	300 ± 5[b]	300 ± 5[b]	297 ± 5[b]			304	
	(389 ± 5)[b]	(380 ± 5)[b]	(379 ± 5)[b]			364	
	(453 ± 5)[b]	(460 ± 5)[b]	(452 ± 5)[b]			444, 486	
	522 ± 4	(520 ± 5)[b]	(519 ± 5)[b]			519	
	(672 ± 5)[b]	(670 ± 5)[b]	(652 ± 5)[b]				
	(760 ± 5)[b]	(760 ± 5)[b]	(752 ± 5)[b]				
	(866 ± 4)	(875 ± 4)	(867 ± 4)				C=C–C bend[c]
	(892 ± 4)		(889 ± 4)				
968	967 ± 2	(953 ± 2)	(957 ± 2)	957	957	960	ν_4(C–C–H out-of-plane bend)[c]
	(975 ± 2)	965 ± 2	967 ± 2	972	984		C_5-Me stretch[c] or C–C–H out-of-plane bend[e] or C=C–C–H angular deformation[d]
1008	1004 ± 1	1004 ± 1	1007 ± 2	1008	1009	1004	ν_3(C–Me stretch)[d]
	(1025 ± 3)	(1022 ± 2)	(1024 ± 3)		1024		C–Me stretch[c]
	(1072 ± 4)	(1064 ± 4)	(1075 ± 4)				skeletal stretching mode[c]
1158	1154 ± 1	1157 ± 1	1156 ± 1	1159	1157	1154	ν_2(C–C and C=C stretch with C–H bend)[d]
	(1176 ± 2)	(1175 ± 4)	1178 ± 4				
	1194 ± 2	1190 ± 2	(1202 ± 2)	1189			C–C stretch + in-plane C–Me rock[c,e]
	1213 ± 2	1213 ± 2	(1231 ± 3)	1209	1218	1210	
		1263 ± 2					
1276	1270 ± 2	1272 ± 2	1271 ± 1	1276	1275	1269	C–C–H bend + C=C or C–C stretch[c]
	1298 ± 2				1290	1303	
	(1306 ± 3)	(1315 ± 4)	1305 ± 1		1311	1316	
	(1357 ± 3)	1357 ± 4					
			(1375 ± 3)			1377	symm C–Me deformations[c,e]
	(1395 ± 3)	1394 ± 4	1388 ± 3				
	1446 ± 2	1447 ± 2	(1449 ± 2)	1447	1449		asymm C–Me deformations[c]
1523	1511 ± 1	1517 ± 1	1501 ± 1	1525	1500	1494	ν_1(C=C stretch)
	(1550 ± 3)						
	(1575 ± 3)	(1579 ± 4)	(1579 ± 4)				cyclohexene C=C stretch[c]
			(1632 ± 3)				C=O stretch[c]

(b) Vibrational Band Wavenumbers (1600–4200-cm^{-1} Region) of Ovorubin and Some Other Astaxanthin Proteins[a]

ovorubin	*P. insularum* astaxanthin protein[g]	V_{620}[h]	assignt	ovorubin	*P. insularum* astaxanthin protein[g]	V_{620}[h]	assignt
1971 ± 10			$\nu_3 + \nu_4$	(2960)			$2\nu_3 + \nu_4$
2007 ± 9	2010	2015[k]	$2\nu_3$	2988 ± 7	2990		
2121 ± 7	(2140)		$\nu_2 + \nu_4$	3020 ± 3	3040	3014[k]	$2\nu_1$
2158 ± 4	2170	2162 ± 4	$\nu_2 + \nu_3$	(3105)			
2304 ± 4	2320	2308 ± 4	$2\nu_2$	(3160)			$\nu_2 + 2\nu_3$
(2343 ± 7)			ν_2 + 1194	(3300)			$2\nu_2 + \nu_3$
2471 ± 7	2490	2461 ± 7	$\nu_1 + \nu_4$	(3465)			$3\nu_2$
2512 ± 5	2530	2507 ± 5	$\nu_1 + \nu_3$	(3630)			$\nu_1 + \nu_2 + \nu_4$
2658 ± 4	2680	2656 ± 4	$\nu_1 + \nu_2$	(3795)			$\nu_1 + 2\nu_2$
(2710)			ν_1 + 1194	(3990)			$2\nu_1 + \nu_4/2\nu_1 + \nu_3$
(2785)	(2790)	(2786)		(4150)			$2\nu_1 + \nu_2$

[a] Wavenumbers in parentheses refer to broad or weak bands and to unresolved shoulders. [b] Uncalibrated values, estimated error given. [c] Possible assignments, see ref 25, derived for vitamin A derivatives. [d] Possible assignments, see ref 11, derived for linear polyenes. [e] Possible assignments, see ref 27, derived for vitamin A derivatives. [f] Reference 7. [g] Astaxanthin protein (λ_{max} 506 nm; inflections, ca. 485 nm and 545 nm) isolated from the eggs of *Pomacea insularum*, dissolved in 0.05 M tris/HCl, pH 6.5. [h] Astaxanthin protein (λ_{max} 620 nm) isolated from *Velella velella*[9] dissolved in 1 M KCl/0.05 M tris/HCl, pH 6.8. [i] Reference 8: left-hand column, excitation within 460-nm absorption band; right-hand column, excitation within 640-nm absorption band. [j] Reference 8. [k] Uncalibrated values, estimated error in band maxima ±10 cm^{-1}.

If, as suggested, all the bands are derived from astaxanthin, there would appear to be a high degree of similarity between the astaxanthin conformations in this diverse range of complexes. Some differences in conformation of the carotenoid are nevertheless present, as seen if the conformation-sensitive fingerprint regions (1100–1400 cm^{-1}) of the resonance Raman spectra of the complexes are compared (Figure 1a,b); these wavenumber differences are insensitive to $\bar{\nu}_0$.

The off-resonance Raman spectrum of ovorubin (647.1-nm excitation) is weaker by a factor of ca. 20 than that obtained under resonance conditions (530.9-nm excitation). Since this applies to all the well-defined bands in the 500–1600-cm^{-1} region, it is clear that a large number of the observed fundamentals are resonantly exhanced within the contour of the $\pi^* \leftarrow \pi$ transition.

The excitation profiles of the ν_1, $2\nu_1$, ν_2, and $2\nu_2$ bands of ovorubin are given in Figure 2 and of the $\nu_1 + \nu_2$, $\nu_1 + \nu_3$, ν_3, and

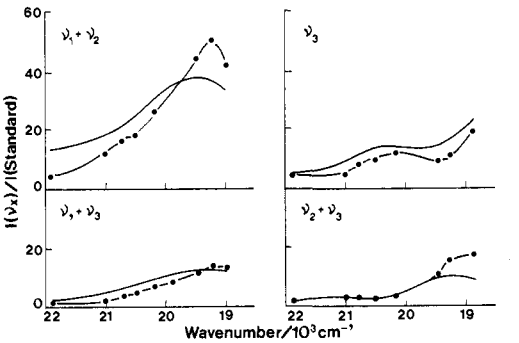

Figure 3. Observed (●) and calculated excitation profiles of the $\nu_1 + \nu_2$, $\nu_1 + \nu_3$, ν_3, and $\nu_2 + \nu_3$ bands of ovorubin. The internal standard is the same as that for Figure 2.

Table II. Resonance Raman Intensities of Different Bands of Ovorubin Calculated from the $\bar{0}$-$\bar{0}$ Transition (I_0) Compared to Those Calculated from a Full set of Vibronic Levels (I_T)[c]

	ν_1	ν_2	ν_3	$\nu_1 + \nu_2$	$2\nu_1$	$2\nu_2$	$\nu_1 + \nu_3$	$\nu_2 + \nu_3$
I_0/I_T[a]	0.7	0.9	1.2	0.9	0.7	1.0	1.0	1.2
I_0/I_T[b]	0.9	1.2	1.4	1.5	1.2	1.8	1.7	2.0

[a] At 530.9-nm excitation. [b] At 543.5-nm excitation, corresponding to exact resonance with the $\bar{0}$-$\bar{0}$ transition. [c] $M_1 = 0.8$, $M_2 = 0.6$, $M_3 = 0.4$, $\Gamma = 1000$ cm^{-1}.

$\nu_2 + \nu_3$ bands of ovorubin are given in Figure 3. The intensities were all measured relative to the same standard so that the profiles show not only the variation of the Raman band intensities with excitation wavenumber but also the relative band intensities.

Calculation of Excitation and Absorption Profiles. Following similar treatments on the carotenoid β-carotene,[17,18] the calculation of excitation and absorption profiles is based on finite displacement parameters for the coordinates associated with the three most intense bands in the resonance Raman spectrum, viz., ν_1 (1511 cm^{-1}), ν_2 (1154 cm^{-1}), and ν_3 (1004 cm^{-1}).

Equation 3 may be reduced to a simple analytical form by ignoring contributions from vibronic levels higher than the $\bar{0}$-$\bar{0}$ level. The analytical equation is strictly true only in the discrete resonance-Raman limit but has been found to be a good approximation under two conditions:[17] (1) The excitation wavenumber is in exact resonance with the $\bar{0}$-$\bar{0}$ transition. (2) The half-bandwidths of the vibronic bands are small compared to the wavenumbers of the enabling vibrational modes. The relative intensities of Raman bands attributable to modes a and b may then be related to the displacement parameter M as in eq 10a–c.

$$I(\nu_a)/I(2\nu_a) = 2/M_a^2 \quad (10a)$$

$$I(\nu_a)/I(\nu_b) = (M_a/M_b)^2 \quad (10b)$$

$$I(\nu_a + \nu_b)/I(\nu_a) = M_b^2 \quad (10c)$$

These equations have been used with the data obtained at 530.9 nm to give the following values for the shift parameters of ν_1, ν_2, and ν_3: $M_1 = 0.8$, $M_2 = 0.6$, and $M_3 = 0.4$. Since both conditions are not followed exactly, the values obtained are approximate, but they represent starting values that then can be optimized to obtain the best fit to the observed profiles.

Table II shows the intensities of the Raman bands calculated by using the $\bar{0}$-$\bar{0}$ transition only, compared to those calculated by using a full set of vibronic levels. The correspondence seems to be better at 530.9 than at 543.5 nm. This is due to a fortuitous cancellation (at 530.9 nm) of the contributions from higher vibronic levels by the second term in eq 3. The best fit to the experimental data was obtained for $M_1 = 0.65$, $M_2 = 0.65$, $M_3 = 0.4$, and $\Gamma = 1000$ cm^{-1}, with the results shown in Figures 2 and 3. The absorption profile (Figure 4) was used to obtain the damping constant Γ for which a variation of 10% from the quoted value had a negligible effect on the fit.

As may be seen from the diagrams, there is some discrepancy between the calculated and measured profiles. By varying M_1 and M_2 from 0.55 to 0.75 and M_3 from 0.3 to 0.5, we may improve the fit to some of the profiles but only at the expense of others.

Although the absorption profile may also be fitted excellently to the values $M_1 = 0.7$, $M_2 = 0.4$, $M_3 = 0.8$, and $\Gamma = 1000$ cm^{-1}, the excitation profiles of the various Raman bands which derive from these values for the parameters do not fit the observed profiles well. This suggests that both absorption as well as excitation profiles should always both be fitted before the appropriate shift parameters are accepted.

Discussion

Excitation and Absorption Profiles. The shapes of the excitation profiles were much easier to simulate than the relative intensities of the bands attributed to the various modes. Thus it would appear that measurements of the relative intensities of Raman bands are necessary in order to obtain accurate shift parameters.[14,17]

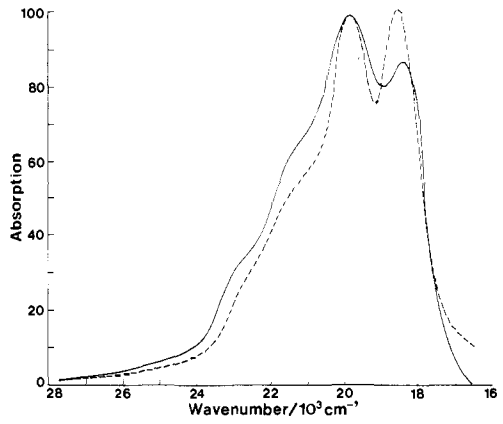

Figure 4. Observed (—) and calculated (---) absorption spectrum of ovorubin, scaled to give the same maximum ordinate values.

The off-resonance spectrum of ovorubin shows conclusively that a larger number of modes of vibration are involved in the $\pi^* \leftarrow \pi$ transition than those taken into account. Although the shift parameters for these extra modes are obviously smaller than for ν_1, ν_2, and ν_3, the total of their effect may not be negligible. To have included these modes in the calculation would have improved the fit to the absorption profile by reducing the intensity of the $\bar{0}$-$\bar{0}$ transition relative to that of the higher levels. However, the inclusion of this large number of modes would not be possible since the number of variables would rise dramatically. For other astaxanthin proteins, it may be possible that the conditions for eq 4 are followed more closely, in which case the shift parameters for a large number of modes could be obtained very easily. At present the assignment of the additional bands cannot be certain for a system as complex as ovorubin. If, however, as probable,[11,25,27] these bands arise essentially from the polyene chain, then the ab initio scheme of calculation originated by Warshel et al.[14] for conjugated molecules would appear to be applicable to the astaxanthin proteins under investigation.

With use of a very simple model,[16] the values of the displacement parameters M_1 and M_2 obtained for β-carotene and astaxanthin[5] have been used to predict the approximate change in double (δ(C=C)) and single (δ(C—C)) bond lengths of the polyene chain in the excited state compared to the values pertaining to the ground state. The relation between δ and M is given in eq 11, where N is Avogadro's number, h is Planck's constant, c

$$\delta = (M/\pi)(Nh/ncm\tilde{\nu})^{1/2} \quad (11)$$

is the velocity of light, m is the mass of the vibrating atom (in amu), $\tilde{\nu}$ is the wavenumber of the appropriate symmetric stretching mode, and n is the number of C=C or C—C bonds in the polyene chain (taken to be 11 and 10, respectively, for ovorubin). The sign of the bond length change cannot, of course, be obtained from this calculation, but molecular orbital calculations indicate that, for β-carotene, on passing from the ground to the excited state, the C=C bonds lengthen whereas the C—C bonds shorten. On these bases, and with $\tilde{\nu}_1 = 1511$ cm^{-1} and $\tilde{\nu}_2 = 1154$ cm^{-1}, the bond length changes for ovorubin on passing from the ground to the resonant excited state are calculated to be δ(C=C) = 0.017 Å and δ(C—C) = −0.020 Å, values which are similar to those found for free astaxanthin (0.020 and −0.025 Å, respectively).[5] A detailed comparison of the results is not possible, however, since the authors[5] neglected the multidimensional form of the vibrational overlap integrals. This has been shown to be erroneous by Warshel et al.[14] and others[17,18] in relation to β-carotene.[28]

Correlation between the Wavenumber of ν_1 and $1/\lambda_{max}$. An empirical correlation between the wavenumber of the ν_1 Raman

(28) The recent time-resolved resonance Raman results on the lowest triplet excited state of *all-trans*-β-carotene suggest that the 1003-cm^{-1} band rather than the 1157-cm^{-1} band, in the ground electronic state, may be more accurately described as the C-C stretching mode. R. F. Dallinger, J. J. Guanci, W. H. Woodruff, and M. A. J. Rodgers, *J. Am. Chem. Soc.*, **101**, 1355 (1979).

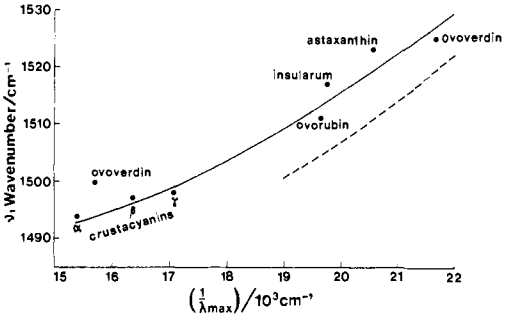

Figure 5. Plot of the ν_1 band wavenumber against $1/\lambda_{max}$ for a number of astaxanthin proteins. The dotted curve represents Rimai's correction.[11]

band and $1/\lambda_{max}$ has been noticed by Rimai et al. for polyenes of increasing chain length.[11] More recently, this correlation has been taken to reflect the extent of π-electron delocalization along the polyene chain for a number of carotenoids[26] and carotenoproteins.[7,8] Although there is good evidence to suggest that this is the case,[10] the plot used depends on the number of atoms in the chain.

The mode of binding of astaxanthin in astaxanthin proteins has been the subject of some controversy.[2,8,12,29] Carey et al.[8] have used the ν_1 vs. $1/\lambda_{max}$ correlation of Rimai to argue that the bathochromic shift in the absorption spectra of astaxanthin in the crustacyanins and ovoverdin (640-nm site) arises from polarization of the carotenoid which gives rise to increased π-electron delocalization in the astaxanthin. These authors reject the possibility of twisting about double bonds of the polyene chain, proposed by Buchwald and Jencks,[29] as the cause of the bathochromic shift in the crustacyanins. A polarization mechanism for the spectral characteristics of the *Asterias rubens* acetylenic astaxanthin protein has also been discussed by Shone.[12]

A plot of ν_1 vs. $1/\lambda_{max}$ for ovorubin and a number of other astaxanthin proteins is shown in Figure 5. The number of atoms in the polyene chain is thus fixed and can no longer be a factor affecting the plot.

In view of the possible diversity of astaxanthin environments in these complexes, any correlation between ν_1 and $1/\lambda_{max}$ would seem surprising, especially since it is probable that their characteristic absorption spectra result not from a single factor but from the interplay of a number of effects.[30] Nevertheless, some kind of correlation between ν_1 and $1/\lambda_{max}$ is evident in Figure 5, although a broader range of astaxanthin proteins is clearly needed to be certain on this point. Thus increased π-electron delocalization for complexes of increasing $1/\lambda_{max}$ would seem, from the resonance Raman data, to be a likely major contributing factor to their spectral characteristics. However, we must stress that until the effect of a C=C twist on the vibrational dynamics of astaxanthin is known,[31] twisting about double bonds of the polyene chain cannot be excluded as a possible mechanism for the bathochromic spectral shifts of the carotenoid in the complexes; indeed such a twist may well lead to a reduction in the wavenumber of ν_1. As stated previously, the essence of the difficulty lies in trying to correlate the Raman band wavenumber, which is solely an electronic ground-state property, to the absorption maximum which contains information on the electronic excited state. It is hoped that further resonance Raman studies, particularly with the proteins combined with synthetic carotenoids, may reveal finer details of carotenoid–protein interaction.

Conclusion

The resonance Raman spectrum of ovorubin, excited by irradiating within the contour of the $\pi^* \leftarrow \pi$ transition of the astaxanthin chromophore, appears to be dominated by vibrational modes arising from the astaxanthin part of the molecule. The profile of the $\pi^* \leftarrow \pi$ absorption band and the excitation profiles (including relative intensities) of some bands involving the polyene chain have been simulated, with some success, by using a simple model applied previously to free carotenoids. These results indicate that more complex models,[14] based on the analysis of conjugated systems, may also be applicable to astaxanthin proteins.

For a number of astaxanthin proteins, as suspected previously,[8] the Raman band wavenumber of the predominantly C=C stretching mode is correlated to the wavenumber of the $\pi^* \leftarrow \pi$ absorption band. As yet, however, it is not clear whether the existence of this correlation can be taken to mean that the absorption spectra exhibited by the astaxanthin proteins is a function only of the extent of π-electron delocalization along an undistorted polyene chain or whether other factors (such as possible distortion of the polyene chain) are important.

A complication, not treated in the above analysis, is the possibility of normal modes changing their internal coordinate character upon electronic excitation. This matter, as well as that of the significance of possible changes in vibrational overlap integrals with wavenumber changes of fundamentals between the ground and excited electronic states, will be considered in a future publication.

Acknowledgment. The authors thank the Science Research Council and the University of London Intercollegiate Research Service for financial support.

(29) M. Buchwald and W. P. Jencks, *Biochemistry*, **7**, 844 (1968).

(30) Note the related discussion for rhodopsin: M. A. Gawinowicz, V. Balogh-Nair, J. S. Sabol, and K. Nakanishi, *J. Am. Chem. Soc.*, **99**, 7720 (1977).

(31) Isomerization to a cis form of the carotenoid would result in an increase in the wavenumber of ν_1, as clearly revealed experimentally for the carotenoids bound to reaction centers of purple, nonsulfur, photosynthetic bacteria. M. Lutz, I. Agalidis, G. Hervo, R. J. Cogdell, and F. Reiss-Husson, *Biochim. Biophys. Acta*, **503**, 287 (1978). A twist about the double bonds of the carotenoid, in the manner suggested by Buchwald and Jencks,[29] contrasts with this situation and would be expected to lead to a decrease in the wavenumber of ν_1.